10

The influence of the combined additive KMnO$_4$ and NH$_4$I on the photosensitive properties of PbS films

© L.N. Maskaeva [1,2], A.V. Beltseva [1], O.S. Yeltsov [1], I.V. Baklanova [3], I.A. Mikhailov [4], V.F. Markov [1,2]

[1] Ural Federal University after the first President of Russia B.N. Yeltsin, Yekaterinburg, Russia
[2] Ural Institute of State Fire Service of EMERCOM of Russia, Yekaterinburg, Russia
[3] Institute of Solid State Chemistry, Russian Academy of Sciences, Ural Branch, Yekaterinburg, Russia
[4] Institute of Nanotechnology of Microelectronics, Russian Academy of Sciences, Moscow, Russia

e-mail: larisamaskaeva@yandex.ru

PbS, PbS(KMnO$_4$), PbS(NH$_4$I), PbS(KMnO$_4$,NH$_4$I) films with good adhesion to a glass substrate with a thickness of 250 to 490 nm were obtained by chemical deposition. Their composition, morphology, and photosensitive properties have been studied. Comprehensive studies using Raman, IR, and Auger spectroscopy established the presence on the surface of the films of a number of impurity oxygen-containing phases (PbO, PbCO$_3$, PbSO$_4$) and cyanamide PbCN$_2$. A synergistic effect of increasing the photoresponse of PbS films synthesized in the presence of a combination of KMnO$_4$ and NH$_4$I additives was revealed, which is due to the formation of an optically active phase of diiodine pentoxide I$_2$O$_5$ on the crystallite surface. Elemental analysis during layer-by-layer ion etching suggested the formation and incorporation of PbSO$_4$, PbCO$_3$, and PbCN$_2$ into the PbS(KMnO$_4$, NH$_4$I) film, and PbCN$_2$ into the PbS(KMnO$_4$) film.

Keywords: chemical deposition, thin films, lead sulfide, diiodine pentoxide, IR, Raman, and Auger spectroscopy, photosensitive properties, synergistic effect.

Introduction

Due to its unique combination of electrophysical and photovoltaic characteristics the narrow-gap thin-film lead sulfide PbS (0.41 eV at 300 K) is successfully used in various practical applications including creation of photodetectors and photodetector devices with limit threshold characteristics (operating at a room temperature, which is especially important [1–4]), generation of heterostructures for solar cells [5,6], sensors for determination of toxic compounds in the air medium and heavy metals in the water medium [7–9], quantum dots [10]. The successful use of these devices depends on a method of synthesis of lead sulfide with improved functional properties.

The thin-film PbS layers are traditionally produced by using both physical and chemical methods. It is often preferred to select chemical deposition from aqueous solutions in the variety of the methods of synthesis of this compound [3,6–8,10,11–16], characterized by simplicity of technological design, high productivity, cost effectiveness, applicability of the films onto metal, semiconductor and dielectric substrates of any form and sizes. Moreover, many researchers believe [17–19] that the chemically deposited lead sulfide films are ones of the most photosensitive materials used in the visible and near infrared (IR) ranges of the spectrum. However, irrelevant of the method of producing the PbS films with the controllable photovoltaic characteristics, it is important to modify a morphology and structure thereof by annealing in an oxygen-containing

medium at 250−550°C [15,18,20,21] in order to saturate intergranular boundaries with oxygen. A degree of this saturation is quite high. In particular, the known theoretical models [22] assume that oxygen therein is distributed along interphase grain boundaries across the entire depth of the layer contributing to provision of the photoresponse. The authors believe [21] that during annealing oxygen adsorbed on microdefects of the crystallites is absorbed by the lead sulfide grains to form the oxygen-containing phases PbO, PbSO$_4$, PbO·PbSO$_4$, PbSO$_3$. These compounds and the adsorbed oxygen create acceptor levels, which are „traps" for the electrons, thereby optimizing the concentration of majority carriers, thereby resulting in the increase in the photosensitivity of the layers under discussion.

The overwhelming majority of the publications dedicated to the synthesis of the PbS films by the methods of chemical deposition from the solutions resolves an issue of inclusion of oxygen into a surface layer by introducing so-called oxidant substances into the reaction mixture [18,21], in particular, sodium sulfite Na$_2$SO$_3$ [23], hydrogen peroxide H$_2$O$_2$ [24,25], the mixture of potassium persulfate K$_2$S$_2$O$_8$ and H$_2$O$_2$ [1]. In addition to the substances with oxidizing properties, in some cases the photosensitivity is increased by introducing reducing agents into the reaction mixture, for example, hydrazine hydrate N$_2$H$_4$·H$_2$O [26], hydrochloride acid hydroxylamine NH$_2$OH·HCl [27].

Another approach substantially influencing the photovoltaic characteristics of the PbS films is to introduce special dopants into the reaction mixture during chemical

deposition, including slats of some metals, which have an inhibiting function during generation of the lead sulfide phase by enlarging an induction period of the process. In this case, the duration of the induction period can be up to $30-50$ min, during which the PbS films accumulate basic salts and carbonate of lead $PbCO_3$ being formed as a result of absorption of CO_2 from air by the alkali reaction mixture [28,29]. In doing so, there is an increase in probability of the reactions with generation of the phase of the basic lead acetate $2PbO \cdot Pb(CH_3COO)_2 \cdot H_2O$, which is adsorbed on the surface of the PbS film. It can be argued that the function of the oxygen-containing impurities in the lead sulfide film is similar to the function of the basic lead sulfate $nPbO \cdot PbSO_4$, which is generated after high-temperature activation of PbS in order to obtain the photoconductive properties by increasing the life time of the majority carriers [21,30]. Relating to the impact of the oxidizers used during the synthesis, the literature tells us about a significant role of the compounds $PbSO_4$ and PbO formed on the surface of the PbS grains in the generation of the photovoltaic properties [31].

There are much less studies done for using halogens and halogen-containing compounds as sensitizing additives in order to produce the photosensitive films of lead chalcogenides. Thus, E.M. Larramendi et al. [32] believe that the introduction of potassium bromide KBr into the reactor does not provide both the oxygen-containing compounds and bromine in the composition of the PbS film, but influences the morphology of the surface and the opto-electric properties. The study has established the dependence of the photosensitivity on the potassium bromide concentrations, but at the same time it has not mentioned the role of sodium sulfite Na_2SO_3, which is also present in reaction mixture.

One should mention a particularly noteworthy role of iodine among the halogens, which can provide the highest photoresponse of the films of metal chalcogenides to IR radiation during the synthesis or subsequent treatment with involvement thereof. It has been demonstrated earlier [33] that the PbS films chemically deposited in the presence of NH_4I are characterized by a relatively high volt-watt sensitivity to IR radiation and do not require additional operations of sensitizing for it.

It is generally assumed that the photoconductive PbS films consist in a system of crystallites separated by intergranular barriers [34]. Petriz believes that the crystallites must have a size from 0.1 to $1.0 \mu m$ and the width of the intergranular barriers from 0.5 to 2.0 Å [34,35]. Once, Indrea and Barbu demonstrated [36] that the PbS film sensitized to light was a heterogeneous system of the crystallites averagely sized as 320 Å, which were separated by the intergranular barriers ~ 160 Å. The intergranular barriers are the most vulnerable areas in relation to conservation of the chemical composition, taking into account processes at the interphase boundaries related to segregation of the impurities and oxidation thereof [34,37]. According to provisions of the theory of intergranular barriers, the authors [38] have

demonstrated that the dark resistance of the deposited PbS films depended on the number of the barriers between the crystallites. The primary photoelectric effect of increased density of the carriers is the result of light absorption by lead sulfide crystallites, which create the „hole$-$electron" pairs. In particular, the main current carriers are the holes, as the layers discussed in the study have the p-type conductivity. The effects of secondary amplification can be a result of reduction of the intergranular barriers due to capture of the minority carriers (electrons). Acharya and Bose [38] have experimentally demonstrated that the barrier height reduces with illumination. Espevik et al. [21] believe that the photoexcitation results in the capture of electrons near the barriers between grains, thereby reducing the thickness of a depleted layer in the grain and increasing a tunnel coefficient of current transfer. The similar mechanism was suggested by Aleshin et al. [31].

It is known [39] that in accordance with the phase diagram Pb$-$S lead sulfide has nonstoichiometry across the basic elements caused by some excess of the lead atoms and is a n-type semiconductor due thereto. The authors of [18,40] believe that with introducing either oxygen or oxygen-containing impurities into the film the n-type conductivity can transform to the stable p-type. In accordance with [32,33], during the chemical deposition the introduction of potassium bromide or ammonia iodide also changes the type of conductivity of the PbS films from „n" to „p". On the other hand, as it has been noted in [33], the PbS films deposited in the presence of ammonium iodide NH_4I with the reduction properties do not require the additional operation of photosensitizing and are characterized by the relatively high volt-watt sensitivity to IR radiation.

The researchers of [17,21,32] believe that the high photosensitivity in the doped PbS films is necessitated by inversion of the type of conductivity from the electron one to the hole one ($n \rightarrow p$) and by a high degree of compensation of the impurity levels across the volume of the crystallites. As the authors of [41] have noted,the samples of the films produced from the aqueous solutions the photosensitivity was exhibited only when the content of the oxidant increased to such a level that the surface of the n-type crystallites showed the acceptor states (formed by oxygen or the oxygen-containing impurity), which capture the electrons out of the volume of the crystallites. Thus, once [1], it has been established that the highest photoresponse of the chemically deposited PbS films corresponded to the content of $15-26$ mass% of lead sulfate $PbSO_4$ therein. Using the Auger spectroscopy, Mohamed et al. [42] have demonstrated the presence of oxygen and carbon both at the surface of and across the volume of the photosensitive films of lead sulfide, which, they believed, was due to generation of the basic lead acetate $2PbO \cdot Pb(CH_3COO)_2 \cdot H_2O$ and lead cyanamide $PbCN_2$ formed as a result of decomposition of the chalcogenator.

So, as it follows from the given literature, the photosensitive properties of the lead sulfide films are much determined by a physical & chemical nature of the dopants and

specific features of their involvement in the photosensitivity mechanism. Moreover, the crucial role is played by the generation of the compounds at the interphase boundary rather than across the volume of the layer. In particular, oxygen adsorbed on the microdefects of the crystallites is absorbed by the grains of lead sulfide with generation of the oxide phases PbO, PbSO$_4$, PbO·PbSO$_4$, PbSO$_3$ [21,30], PbCO$_3$ [28,29] and the emergence of inversion channels in a subsurface area of the crystallites with the *p*-type conductivity and the tunnel mechanism of transfer of holes through the intergranular interlayers [43].

In the case of doping the lead sulfide with iodine, we have assumed in [33] that the self-compensation mechanism of the photosensitivity was possible due to generation of point defects in the form of the impurity PbI$_2$, which contributed to the inversion of the $(n \rightarrow p)$-type conductivity with optimization of the concentration of the charge carriers in the semiconductor layer [44].

Thus, there are now contradictory representations about the nature of the compounds in the composition of the chemically deposited thin films of lead sulfide, which play an important role in provision of the photosensitive properties thereof. The literature has been analyzed to reveal the ambiguity of the results, which were available for the doping impact and the influence of the additives of an oxidation or reduction nature on the structural and morphological characteristics, the semiconductor and function properties of the PbS films. At the same time, the literature contains no data on chemical deposition of the lead sulfide films in the exemplified presence of such a characteristic oxidizer as potassium permanganate KMnO$_4$.

Therefore, for understanding the nature of the photoresponse of the PbS films and its relation to the structural and electrophysical characteristics of the compounds under discussion, as well as for practical implementation of the results obtained, the highly-effective optoelectronic devices are created with paying large interest to producing the layers by chemical deposition with substances of various oxidation-reduction properties, simultaneously present in the reaction mixture. In this relation, the present study has comparatively investigated the morphology, the semiconductor and photovoltaic properties of the PbS films, which are chemically deposited in the presence of the individual additives NH$_4$I and KMnO$_4$, and with the combination thereof as well.

Experiment procedure

The lead sulfide films were produced by chemical deposition from the aqueous solutions as per the following reaction

$$Pb^{2+} + (NH_2)_2CS + 2OH^- = PbS + H_2CN_2 + 2H_2O. \quad (1)$$
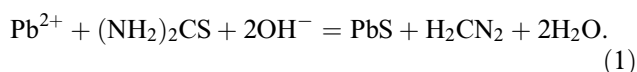
The ammonium & citrate reaction mixture for film deposition included the lead acetate Pb(CH$_3$COO)$_2$, the sodium citrate Na$_3$C$_6$H$_5$O$_7$, the ammonium hydroxide NH$_4$OH and thiourea (NH$_2$)$_2$CS [29]. The films produced from this

mixture without introduction of the additional additives was designated as PbS(0). The second option of the synthesis included additional introduction of 0.15 mol/l of ammonium iodide NH$_4$I into the reaction mixture, thereby resulting in producing the layers PbS(NH$_4$I). In the third option, the reaction mixture contained from 0.01 to 10 mmol/l of the oxidizer as potassium permanganate KMnO$_4$, and the films deposited in its presence were designated as PbS(KMnO$_4$). The layers deposited with addition of the combination of KMnO$_4$ (0.01−5.0 mmol/l) and NH$_4$I (0.15 mol/l) were designated as PbS(KMnO$_4$, NH$_4$I). The films were deposited at 353 K during 90 min to pre-degreased substrates made of a slide (72.2% SiO$_2$, 14.3% Na$_2$O, 1.2% K$_2$O, 6.4% CaO, 4.3% MgO, 1.2% Al$_2$O$_3$, 0.03% FeO, 0.3% SO$_3$) using the liquid thermostat „TS-TB-10" designed to ensure the temperature maintaining error of ± 0.1 K. The thickness of the films produced were determined using the interference microscope MII-4M with the error of 10%.

The morphology and the elemental composition of the films were studied by means of the scanning election microscope Scanning Electron Mucroscope Tescan Vega 4 LMS with the energy-dispersive add-on (EDS) Oxford Xplore EDS−AZtecOne. The elemental composition of the film was determined with the error of about 10%. The particle size was determined using the Measurer software with further data processing in the Grapher 9.6 application package.

The spectra of the Raman scattering (RS) of the samples were recorded at the room temperature within the range of the wave numbers of $50−1200$ cm^{-1} using the confocal Raman microscope RenishawInViaReflex ($\lambda_{laser} = 532$ nm, 1 s, $P = 50$ mW). The infrared spectra of the synthesized films were recorded by the Fourier spectrometer Bruker Alpha, the ATR attachment (ZnSe), within the range of $500−4000$ cm^{-1} with the resolution of 4 cm^{-1}. The Auger spectra of the films under study were obtained in the Auger-electron microscope Jamp-9510F (produced by JEOL) with an inclination angle of the sample in relation to the electron beam $30°$ at the accelerating voltage of 10 keV before and after ion etching. When profiling, a diameter of the electron beam was about 100 μm. The depth distribution profile was obtained by using an ion gun with the argon ion energy of 2000 eV. The rate of etching the samples being investigated was 63 nm/min. The method error was $\sim 10\%$.

The photosensitive properties of the films were studied using sensitive cells sized as 5×5 mm and produced based thereon, which had electrochemically applied ohmic nickel contacts. The volt sensitivity of the synthesized films was measured on a special bench K.54.410 with a source of IR radiation in the form of the black body (BB) with the temperature of 573 K, at the sensitive cell irradiance of 10^{-4} W/cm^2, the radiation modulation frequency of 800 Hz and the offset voltage of 50 V. The photoresponse was recorded in the form of the voltage drop at a consistent load resistance.

The conductivity type of the deposited films was determined by checking the sign of thermo-emf in experiments
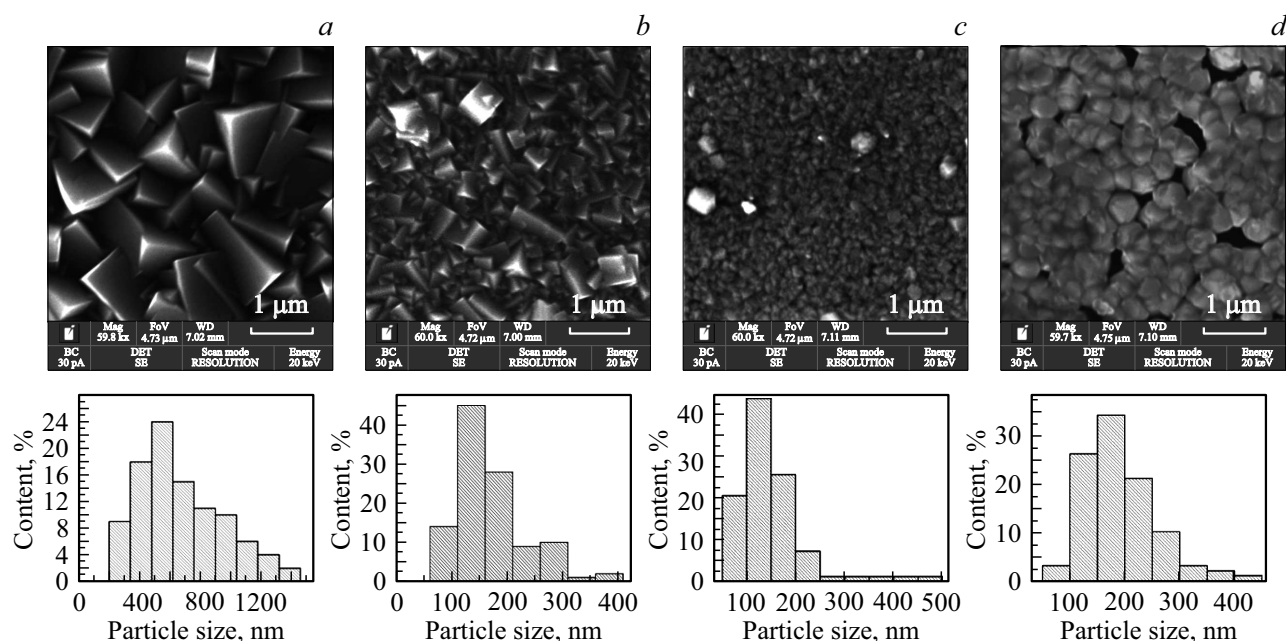
Figure 1. Electron microscopic images of the films PbS(0) (*a*), PbS(KMnO$_4$) (*b*), PbS(NH$_4$I) (*c*), PbS(KMnO$_4$, NH$_4$I) (*d*), chemically deposited out of the solutions containing 0.15 mol/l NH$_4$I and 1.0 mmol/l KMnO$_4$, and histograms of size distribution of the particles.

Characteristic frequency (in cm^{-1}) of the absorption bands of the surface compounds in the films PbS(0), PbS(NH$_4$I), PbS(KMnO$_4$), PbS(KMnO$_4$, NH$_4$I)

PbS(0)	PbS(NH$_4$I)	PbS(KMnO$_4$)	PbS(KMnO$_4$, NH$_4$I)	Compound, bound vibrations	Literature data
759	732	758	744	PbO	718.4 [55]
	833		856	I$_2$O$_5$	835−809 [61]
942	947			PbSO$_4$	966 [57]
	1297		1259	Valent vibrations of the bond C=S	1060−1400 [59]
			1455	PbCO$_3$	1435 [58]
1538	1527	1571		CH$_3$COO$^-$	1578 [60]
		1747	1746	PbCO$_3$	1741 [58]
1946	1945	1938	1941	PbCN$_2$	1950 [56]
2228		2285		Valent vibrations C≡N	2260−2240 [59]
2349		2390		Valent vibrations C≡N	2300−2250 [59]
		3161		Valent vibrations of the NH group	3100 [60]
	3741			Free hydroxyl OH group	3600-2700 [59]

Note. It is more reasonable to associate the obtained results with the absorption bands in the spectra of adsorption products of carbon dioxide and carbonate ions on the oxide surfaces. Thus, [59] states that the vibration frequency of the C−O bridge carbonate groups in the spectrum of one of the oxide systems is observed at 1750 cm^{-1}, so are the antisymmetric valent vibrations in the CO$_3^{-2}$ — at 1430 cm in the $^{-1}$ structure. The paper [60] also demonstrates that the bands within this region are observed, in particular, in the spectra of CO$_2$ adsorbed on a number of metal oxides.

where a temperature gradient was created in the region of probe contacts.

Experimental results and discussion thereof

At fixed concentrations of components in the citrate & ammonium reaction bath chemical deposition has produced the mirror films PbS(0), PbS(KMnO$_4$), PbS(NH$_4$I), PbS(KMnO$_4$,NH$_4$I) with good adhesion to glass substrates of the thickness of 490, 380, 280 and 250 nm, respectively.

The morphology of the synthesized films with an observed single-mode character of grain size distribution evolves as shown on the electron microscopic images (Fig. 1). Thus, the film PbS(0) (Fig. 1, *a*) consists of well faceted fitted crystallites averagely sized as 400−800 nm ($\sim$ 70%), oriented both as (111) and (220). The introduction of 1.0 mmol/l KMnO$_4$ into the reactor does not change the shape of the grains, but results in reduction of their sizes to 100−200 nm ($\sim$ 75% of the total number) and emergence of the $\sim$ 14% nanoparticles (Fig. 1,*b*). The films PbS(NH$_4$I) and PbS (KMnO$_4$,NH$_4$I) substantially differ from the above in disappearance of fine faceting of the crystallites. The iodine-doped lead sulfide PbS film (NH$_4$I) is a quite homogeneous microstructure with an average grain size of 100−200 nm ($\sim$ 70%) and single globules of a diameter up to 500−600 nm with the content of $\sim$ 20% nanoparticles (Fig. 1, *c*). When the reaction bath simultaneously contains KMnO$_4$ and NH$_4$I, the thin-film layer is formed from the 100−250 nm grains ($\sim$ 80%) with reduction of the portion of the nanoparticles down to $\sim$ 3% (Fig. 1, *d*). The microimages of the PbS films (KMnO$_4$, NH$_4$I) visually demonstrate no substrate coating, but it signifies not a lack of the film on these portions, but only reduction of its thickness.

The content of the basic elements (Pb, S, O, I) in the films PbS(0), PbS(KMnO$_4$), PbS(NH$_4$I), PbS(KMnO$_4$, NH$_4$I) was determined using the elemental energy-dispersive microanalysis across the entire area of their surface. The undoped PbS film exhibits the similar content of atoms of lead (50.1 at.%) and sulphur (49.9 at.%). In turn, the PbS films(KMnO$_4$) produced with introducing the oxidizer into the reaction bath exhibit reduction of the content of these elements to 45.9 and 44.4 at.%, respectively, and oxygen of up to 3.6−9.7 at.%. The elemental analysis of the iodine-doped PbS layer (NH$_4$I) indicates that both separate globules and the surface consist in predominantly lead and sulphur, whose content was 49.8 and 48.3 at.%, respectively, while the iodine content was $\sim$ 1.9 at.%. However, it was difficult to obtain more exact information on the elemental composition of the PbS films (KMnO$_4$, NH$_4$I) due to their small thickness and visually observed heterogeneities (Fig. 1, *d*).

The produced films PbS(0) had the *n*-type conductivity. The inclusion of oxygen into the PbS film (KMnO$_4$) did
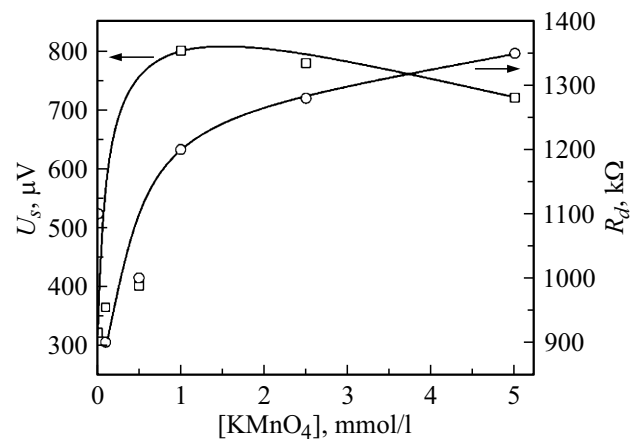

Figure 2. Dependence of the volt sensitivity U_S and the dark resistance R_d of the 5 $\times$ 5 mm cells based on the PbS films (KMnO$_4$, NH$_4$I) on the concentration of KMnO$_4$ in the reaction bath at the content of 0.15 mol/l NH$_4$I.

not change the conductivity type. Measuring the thermo-emf sign allowed recording the stable hole semiconductor type of conductivity in the doped layers PbS(NH$_4$I) and PbS(KMnO$_4$, NH$_4$I).

Fig. 2 shows the influence of the combination of the dopants with simultaneous introduction of KMnO$_4$ and NH$_4$I nfluenceinto the reaction bath on the functional properties of the thin-film PbS layers (KMnO$_4$, NH$_4$I), in particular, on their volt sensitivity U_S and the dark resistance R_d. As it is clear from the figure, the PbS film (NH$_4$I) deposited from the solution with added 0.15 mol/l NH$_4$I, but without KMnO$_4$, has a value of the volt sensitivity at the given conditions at 320 μV. Additional introduction of KMnO$_4$ into the solution contributes to substantial increase in the film photoresponse, wherein the dependence of the volt sensitivity on the potassium permanganate's concentration is of an extreme nature. The maximum value of U_S of $\sim$ 800 μV corresponds to the concentration of KMnO$_4$ of 1.0 mmol/l. Further increase in the content of KMnO$_4$ is accompanied by gradual reduction of U_S to $\sim$ 700 μV at 5.0 mmol/l, so is at 10 mmol/l to 600 μV. It can be assumed that the film deposited at 1.0 mmol/l KMnO$_4$ and 0.15 mol/l NH$_4$I in the reactor has the concentration of the primary carriers (holes), which is close to the optimum one, due to the presence of the impurity phases and specific features of its microstructure. Thus, the introduction of the combined additive KMnO$_4$ and NH$_4$I increases the volt sensitivity of the PbS films (KMnO$_4$, NH$_4$I) almost two times, indicating a synergistic effect. As for the dependence $R_d = f([\text{KMnO}_4])$, then we should note the growing dark resistance from 900 to 1300 kΩ and to 1450 kΩ (10 mmol/l) with the increase in the potassium permanganate's concentration in the reaction bath.

Larramendi et al. [32] have noteworthily explained a similar extreme dependence of the PbS photosensitivity on the potassium bromide KBr in the reaction bath, which is
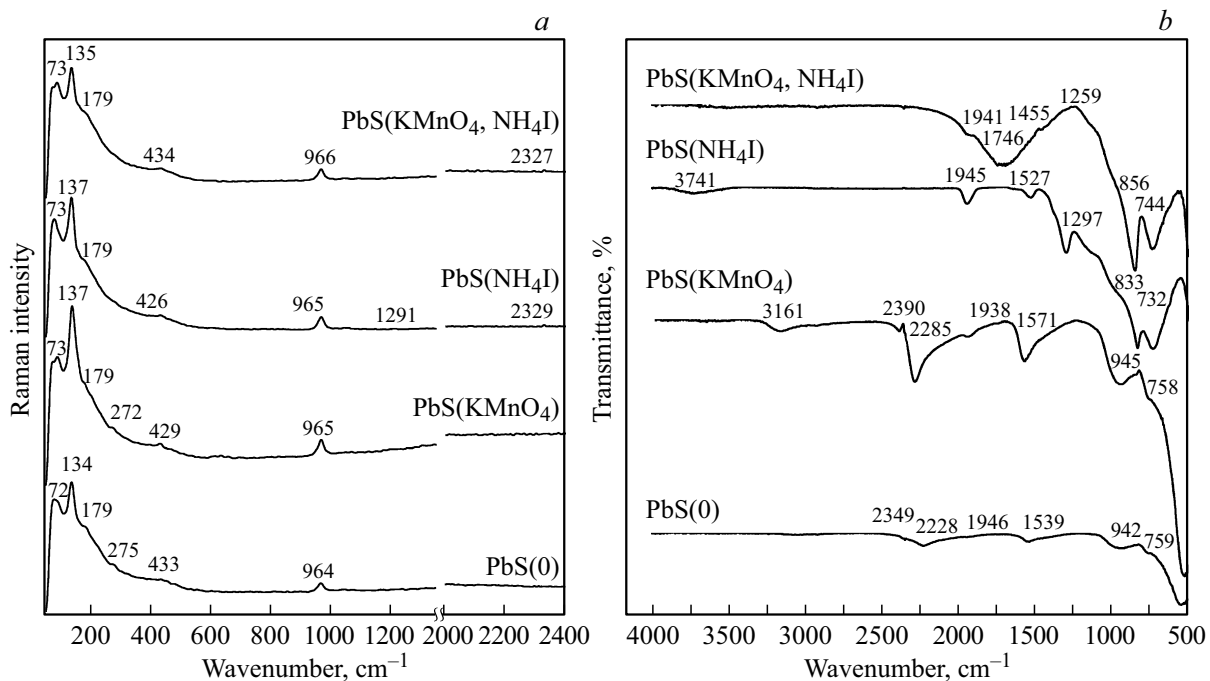
Figure 3. Spectra of Raman scattering (*a*) and IR transmittance spectra (*b*) of the films PbS(0), PbS(NH$_4$I), PbS(KMnO$_4$), PbS(KMnO$_4$, NH$_4$I).
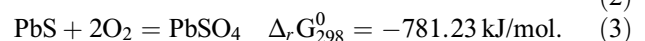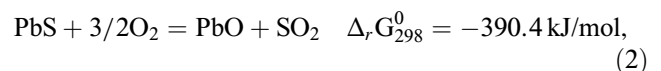
defined by the surface film characteristics rather than the volume ones, in particular, by disorder of the inversion channels at the grain boundaries. Moreover, the bromine impurity in the composition of the polycrystalline PbS film was not found, and only modification of the morphology of the layer surface was observed.

In order to identify the impurity compounds both at the surface and across the volume of the semiconductor layers PbS(0), PbS(KMnO$_4$), PbS(NH$_4$I), PbS(KMnO$_4$, NH$_4$I), we have applied a set of investigation methods including RS, IR and Auger spectroscopy.

Fig. 3, *a* shows the RS spectra of the film samples under discussion at the room temperature in the range of the wave numbers 50−1200 cm^{-1}. As it is known, a position and a form of the lines within the RS spectra depend on a molecular structure of the compound. The RS spectra of the films being investigated exhibit six oscillating active Raman modes around 72−73, 134−137, 179, 275, 426−433, 964−966 cm^{-1} [45,46]. The intensive peak 134−137 cm^{-1} reflects a combination of longitudinal and transverse acoustic modes (LA + TA) [47−49]. We have also recorded the mode at the lower frequency (72−73 cm^{-1}), which can be attributed to the transverse optical modes (TO) [50,51]. The observed weak line of Raman scattering in the PbS structure within the frequency range 179−181 cm^{-1} relates to the longitudinal optical mode (LO), while the line at 426−434 cm^{-1} comes from the first overtone of the basic longitudinal optical (LO) phonon modes of PbS (2LO) [52]. As per the data of [53], the mode around 272−275 cm^{-1} belonging to PbO is recorded only in the RM spectra of the films PbS(0) and

PbS(KMnO$_4$). The valent symmetrical vibrations ν_1 SO$_4^{2-}$ (PbSO$_4$) are due to the mode 964−966 cm^{-1} [54], which is observed in the RS spectra of all the synthesized film samples.

The impurity phases (PbO, PbSO$_4$) identified by Raman-scattering spectroscopy can be explained by oxidation of lead sulfide:

$$\text{PbS} + 3/2\text{O}_2 = \text{PbO} + \text{SO}_2 \quad \Delta_r\text{G}_{298}^0 = -390.4\,\text{kJ/mol},$$
$$(2)$$
$$\text{PbS} + 2\text{O}_2 = \text{PbSO}_4 \quad \Delta_r\text{G}_{298}^0 = -781.23\,\text{kJ/mol}. \quad (3)$$

It should be noted that the generation of lead sulfate is thermodynamically more advantageous to the generation of the oxide, which is confirmed by the RS spectra exhibiting the more intensive peak at the frequency 964−966 cm^{-1} and the weak peak in the low-frequency region 272−275 cm^{-1}. Thus, the RS spectra were useful in identifying only two impurity phases — PbO and PbSO$_4$ available in the films, which agrees with the data given in [21,30].

Results of the IR spectroscopy should be also involved in order to get a full set of the normal vibrations and, consequently, a position of the oscillating levels of the bond energy in the samples formed on the surface. Fig. 3, *b* shows the IR spectra of the film samples PbS(0), PbS(NH$_4$I), PbS(KMnO$_4$), PbS(KMnO$_4$, NH$_4$I) containing a number of characteristic absorption bands to establish the chemical composition thereof.

The table references the vibrational frequencies found in the IR spectra of the films discussed and in the literature sources. All the film samples under discussion have
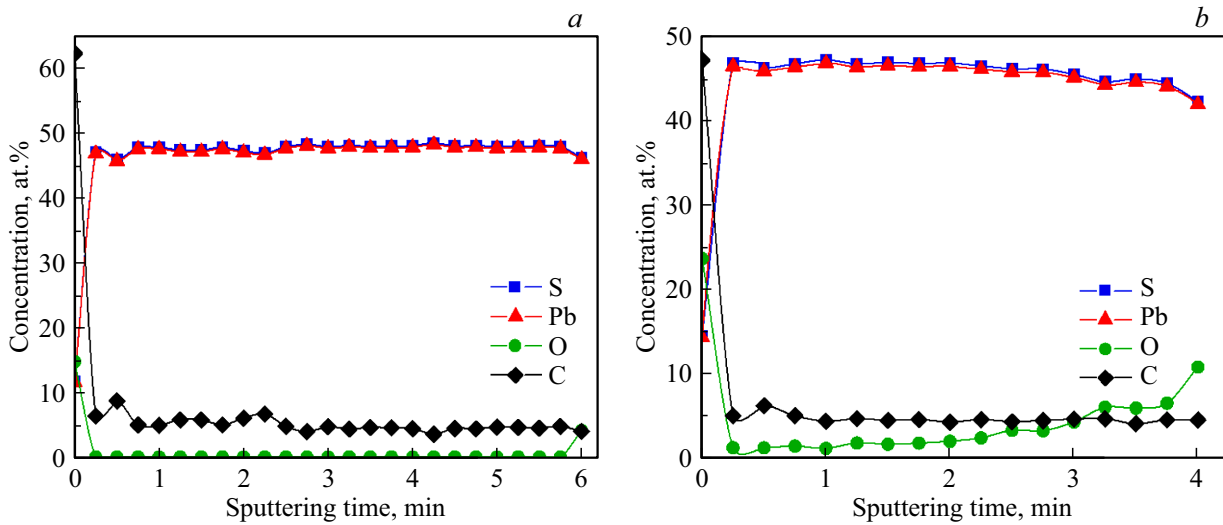
Figure 4. Concentration profiles of element distribution across the thickness of the PbS films(KMnO$_4$) and PbS(KMnO$_4$,NH$_4$I) deposited onto the glass substrates out of the reaction mixtures, which contain (*a*) 1.0 mmol/l KMnO$_4$, (*b*) the combination of 1.0 mmol/l KMnO$_4$ and 0.15 mol/l NH$_4$I.

the most expressed absorption lines with the maximums 732−759, 1938−1946 cm^{-1}, which correspond to the PbO oxide and the cyanamide PbCN$_2$ as per the literature data (718.4 cm^{-1} [55] and 1950 cm^{-1} [56]) The lead cyanamide PbCN$_2$ is resulted from hydrolytic decomposition of thiourea in the ammonium & citrate reaction mixture with pH 12.2,which occurs as per the reactions

$$N_2H_4CS = H_2S + H_2CN_2, \qquad (4)$$

$$H_2CN_2 + Pb^{2+} + 2OH^- = PbCN_2 + 2H_2O. \qquad (5)$$
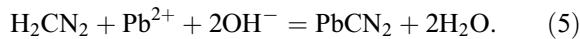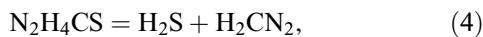
As in the RS spectra, the presence of lead sulfate PbSO$_4$ can be judged by the absorption bands 943 cm^{-1} (PbS(0)) and 947 cm^{-1} (PbS(KMnO$_4$)), which characterize the valent vibrations of the SO$_4^{2-}$-ion with slight offset to the low-frequency region as compared to the frequency of 966 cm^{-1} given in [57].
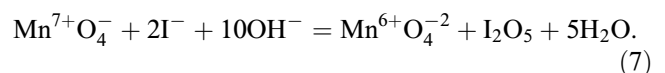
The IR spectra of the PbS films(KMnO$_4$), PbS(KMnO$_4$, NH$_4$I) contain the absorption bands 1747, 1455 and 1746 cm^{-1}, which can be supposedly attributed to lead carbonate resulted from absorption of CO$_2$ from air by the alkali reaction mixture. In terms of their values, the recorded frequencies are close to 1741 and 1435 cm^{-1} as given in [58] for carbonate. However, probably, it is more reasonable to identify the obtained results with the absorption bands in the spectra of adsorption products of carbon dioxide and carbonate ions on the oxide surfaces. Thus, [59] states that the vibration frequency of the C−O bridge carbonate groups in the spectrum of one of the oxide systems is observed at 1750 cm^{-1}, so are the antisymmetric valent vibrations of the C=O — at 1450 cm^{-1} in the CO$_3^{-2}$ structure. The paper [60] also demonstrates that the bands within this region are observed, in particular, in the spectra of CO$_2$ adsorbed on a number of metal oxides.

The valent vibrations in C≡N at the frequencies of 2228, 2285 cm^{-1} and 2349, 2390 cm^{-1}, which are identified in the IR spectra of PbS(0) and PbS(KMnO$_4$), are close to the values of 2260−2240 and 2300−2250 cm^{-1} of [61]. The surface PbS layer (KMnO$_4$) exhibits recorded valent vibrations of the N−H group at the frequency of 3161 cm^{-1} [60] and a weak-intensity of the absorption band at 3741 cm^{-1}, which is responsible for the free hydroxyl OH group [61]. The absorption bands in the region of 1527−1571 cm^{-1} characterize the vibrations of the group of the CH$_3$COO$^-$acetate ions [62] on the surface of the film samples PbS(0), PbS(NH$_4$I), PbS(KMnO$_4$).

Let us consider specific features of the IR spectra of the photosensitive film samples PbS(NH$_4$I) and PbS(KMnO$_4$, NH$_4$I). In the frequency range of 835−809 cm^{-1} [63] the spectrum of the PbS film (NH$_4$I) exhibits a detected absorption band at the vibration frequency of 833 cm^{-1}, which is characteristic for diiodine pentoxide I$_2$O$_5$. This light-sensitive phase is resulted from emergence of the PbO impurity phase, which in an alkali medium acts as the oxidizer of the iodide ions I$^-$ in the reaction

$$4Pb^{2+}O + 2I^- + 2OH^- = 4Pb^0 + I_2O_5 + H_2O. \qquad (6)$$
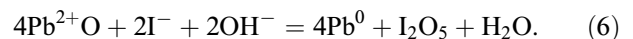
The studies have shown that the addition introduction of ammonium iodide and the oxidizer in the form of KMnO$_4$ as well is accompanied by shift of the absorption band to the high-frequency region from 833 to 856 cm^{-1} and by increase in the intensity thereof. It can be interpreted as an increase in the content of I$_2$O$_5$ on the surface of the PbS film (KMnO$_4$, NH$_4$I) due to additional oxidation of the iodide ions I$^-$ by the permanganate ions MnO$_4^-$ as per the following reaction

$$Mn^{7+}O_4^- + 2I^- + 10OH^- = Mn^{6+}O_4^{-2} + I_2O_5 + 5H_2O. \qquad (7)$$

Another specific feature of the IR spectra of the films PbS (NH_4I) and PbS($KMnO_4$, NH_4I) is the presence of valent vibrations of the C=S bond [61]: the more intensive narrow peak at the frequency of $1297 \, cm^{-1}$ and the weak one at the frequency of $1259 \, cm^{-1}$.

Thus, the obtained results indicate that the introduction of the combined oxidizer $KMnO_4$ and NH_4I originates the synergistic effect of their impact related to more intensive generation of the optically active phase I_2O_5. Probably, it is one of the main reasons of the increased photoresponse for the deposited films PbS($KMnO_4$, NH_4I) as compared to PbS(NH_4I) synthesized using only the NH_4I additive.

Fig. 4 shows profiles of distribution of the basic and impurity elements (Pb, S, C, O) across the depth of the layer PbS ($KMnO_4$) and PbS($KMnO_4$, NH_4I), which are produced by layer-by-layer Auger electron spectroscopy. The elemental analysis of the subsurface layers of the films PbS($KMnO_4$) and PbS($KMnO_4$, NH_4I) has shown that they included a quite large amount of carbon — 62.2 and 47.4 at.%, respectively, at the content of oxygen of 14.7 and 23.8 at.%. That is, the NH_4I additive stimulates the generation of the oxygen-containing phases in the surface PbS layer ($KMnO_4$, NH_4I). Carbon is present both due to surface contaminations and the impurity of final and intermediate products of decomposition of thiourea during the synthesis. Besides, there is high probability of generation of lead sulfate $PbSO_4$ as a result of oxidation of the sulfide of this metal [1] as well as of lead carbonate $PbCO_3$ due to absorption of carbon dioxide from air by the alkali reaction mixture [28,29].

The content of the basic elements (Pb and S) in the surface PbS layer ($KMnO_4$) is 11.5–11.6 at.%. At the surface of the semiconductor PbS layer ($KMnO_4$, NH_4I) deposited using the combined additive $KMnO_4$ and NH_4I, the content of lead and sulphur is somewhat higher — 14.3–14.7 at.%. After 25-s ion etching of the surface PbS layer ($KMnO_4$) (Fig. 4, *a*) no oxygen is virtually detected, while the content of lead Pb (46.7 at.%), sulphur S (46.9 at.%) and carbon C (~ 4.5 at.% with the deviations of 6.6 and 8.6 at.%) is „plateauing". As for the PbS films ($KMnO_4$, NH_4I) (Fig. 4, *b*), the content of oxygen across the volume (across the film thickness) gradually increases from 1.2 to ~ 6.5 at.%, and the content of carbon is within the range from 4.1 to 6.2 at.%. It can be assumed that the presence of the carbon impurity across the thickness of the PbS film ($KMnO_4$) is related to generation of lead cyanamide $PbCN_2$ during the synthesis as per the reaction (5) (Fig. 4, *a*). With the same content of carbon, the PbS film ($KMnO_4$, NH_4I) (Fig. 4, *b*) is gradually increasing its content of oxygen, and we can assume that the impurity phase $PbCO_3$ is also generated beside the cyanamide $PbCN_2$.

The data obtained for distribution of the impurity elements across the thickness of the PbS film ($KMnO_4$, NH_4I) agree with the results of Auger spectroscopy of the photosensitive PbS as given in the study [43]. The concentration profiles of element distribution in both the films are specifically characterized by the presence of oxygen near the surface of the glass substrate from 4.1 at.% for PbS($KMnO_4$) to 10.8 at.% for PbS($KMnO_4$, NH_4I), which is related to nucleation thereof as per the „hydroxide" mechanism, i.e. with generation of a sublayer of lead hydroxide $Pb(OH)_2$ [33,43].

Conclusion

The chemical deposition has produced the polycrystalline thin films of lead sulfide of the thickness of 250–490 nm on the glass substrates with introducing the sensitizing additives of potassium permanganate, ammonium iodide and the combination thereof. The influence of the said additives on the thickness and the morphology of the synthesized layers has been shown provided that the single-mode nature of the microcrystal size distribution is maintained.

Using the Auger electron spectroscopy, the layer-by-layer-by-layer etching of the layers had produced the profiles of distribution of the basic and impurity elements (Pb, S, C, O), which made it possible to identify lead cyanamide $PbCN_2$ in the films and to assume that lead carbonate $PbCO_3$ was generated in the PbS film ($KMnO_4$, NH_4I).

The IR and RS spectra of the films PbS(0), PbS($KMnO_4$), PbS(NH_4I) and PbS($KMnO_4$, NH_4I) had been analyzed, which made it possible to identify a number of generated compounds of the various composition therein. In particular, the RS spectra have the six oscillating active Raman modes around 72–73, 134–137, 179, 275, 426–433, 964–966 cm^{-1}. The mode near 272–275 cm^{-1}, belonging to PbO is recorded only in the spectra of the films PbS(0) and PbS($KMnO_4$), while the valent symmetrical vibrations of the sulfate ion SO_4^{2-} ($PbSO_4$) (which correspond to 964–966 cm^{-1}) are observed in all the investigated film samples.

The IR spectra of all the samples indicate that they have the impurity phases of lead oxide PbO (732–759 cm^{-1}) and cyanamide thereof $PbCN_2$ (1938–1946 cm^{-1}) as the final product of decomposition of thiourea. This is the first time that the IR spectroscopy of the films PbS(NH_4I) and PbS($KMnO_4$, NH_4I) has established the generation of the phase of diiodine pentoxide I_2O_5 at the frequencies of 833 and 856 cm^{-1}, respectively.

In the presence of the additives of ammonium iodide, PbS(NH_4I) and its combination with potassium permanganate PbS($KMnO_4$, NH_4I), it has established the inversion of the inversion of the conductivity type $n \rightarrow p$ in the deposited layers. It also includes the establishment of the extreme nature of the volt sensitivity of the PbS films ($KMnO_4$, NH_4I) on the addition of potassium permanganate into the solution. The combination of the additives 1.0 mmol/l $KMnO_4$ and 0.15 mol/l NH_4I contributes to increase in the film photoresponse to IR radiation approximately two times as compared to the PbS film (NH_4I) by the synergistic effect, which is due to more significant

generation of the optically active phase of diiodine pentoxide I$_2$O$_5$,

With the results obtained, we can assume that the crucial role in sensing the lead sulfide films synthesized in the study is predominantly played by the presence of the phase I$_2$O$_5$ rather than impurity compounds PbCN$_2$, PbCO$_3$, PbO, PbSO$_4$.

Funding

Conflict of interest

The authors declare that they have no conflict of interest.

References

[1] C. Nacu, V. Vomir, I. Pop, V. Ionescu, R. Grecu. Mater. Sci. Eng. B, **41** (2), 235 (1996). DOI: 10.1016/s0921-5107(96)01611-x

[2] P.M. Khanzode, D.I. Halge, V.N. Narwade, J.W. Dadge, K.A. Bogle. Optik, **226** (1), 165933 (2020). DOI: 10.1016/j.ijleo.2020.165933

[3] S.M. Lee, W. Jang, B.C. Mohanty, J. Yoo, J.W. Jang, D.B. Kim, Y. Yi, A. Soon, Y.S. Cho. Chem. Mater., **30** (21), 7776 (2018). DOI: 10.1021/acs.chemmater.8b03177

[4] T. Li, X. Tang, M. Chen. Coatings, **12**, 609 (2022). DOI: 10.3390/coatings12050609

[5] D.G. Moon, S. Rehan, D.H. Yeon, S.M. Lee, S.J. Park, S.J. Ahn, Y.S. Cho. Sol. Energy Mater. Sol. Cells., **200**, 109963(2019). DOI: 10.1016/j.solmat.2019.109963

[6] D.H. Yeon, B.C. Mohanty, C.Y. Lee, S.M. Lee, Y.S. Cho. ACS Omega, **2** (8), 4894 (2017). DOI: 10.1021/acsomega.7b00999

[7] V.V. Burungale, R.V. Devan, S.A. Pawar, N.S. Harale, V.L. Patil, V.K. Rao, P.S. Patil. Mater. Sci. Pol., **34**(1), 204 (2016). DOI: 10.1515/msp-2016-000

[8] I.V. Zarubin, V.F. Markov, L.N. Maskaeva, N.V. Zarubina, M.V. Kuznetsov. J. Anal. Chem., **72** (3), 327 (2017). DOI: 10.1134/S1061934817030145.

[9] T.V. Beatriceveena, E. Prabhu, A. Sree Rama Murthy, V. Jayaraman, K.I. Gnanasekar. Appl. Surf. Sci., **456**, 430 (2018). DOI: 10.1016/j.apsusc.2018.06.145

[10] V.M. Goossens, N.V. Sukharevska, D.N. Dirin, M.V. Kovalenko, M.A. Loi. Cell Reports Phys. Sci., **2** (12), 100655 (2021). DOI: 10.1016/j.xcrp.2021.100655

[11] B.Yasabu, F. Gashaw. Inter. J. Agric. Natur. Sci., **14**(1), 16 (2021).

[12] U. Chalapathi, S.-H. Park, W.J. Choi. Mater. Sci. Semicond. Process., **134**, 106022 (2021). DOI: 10.1016/j.mssp.2021.106022

[13] U. Chalapathi, S.-H. Park, W.J. Choi. Mater. Sci. Semicond. Process., **136**, 106147 (2021). DOI: 10.1016/j.mssp.2021.106147

[14] B.G. Zaragoza-Palaciosa, A.R. Torres-Duarteb, S.J. Castillo. J. Mater. Sci. - Mater. Electron., **32** (9), (2021). DOI: 10.1007/s10854-021-06702-y

[15] A. Elmadani, R. Essajaia, A. Qachaou, A. Raidou, M. Fahoume, M. Lharch. Adv. Mater. Proces. Techn., **8** (3), 3413 (2022). DOI: 10.1080/2374068X.2021.1970986

[16] A.S. Barona, M.M. Aboodb, K.A. Mohammed. Chalcogenide Lett., **18** (12), 759 (2021). DOI: 10.1088/0034-4885/23/1/301

[17] D. Vankhade, T.K. Chaudhuri. J. Appl. Phys., **127**(17), 175107 (2020). DOI: 10.1063/1.5138908

[18] G.P. Kothiyal, B. Gosh, R.Y. Deshpande. J. Phys. D, **13**(5), 869 (1980). DOI: 10.1088/0022-3727/13/5/022

[19] M.S. Ghamsari, M.K. Araghi, S.J. Farahani. Mater. Sci. Eng. B, **133** (1−3), 113 (2006). DOI: 10.1016/j.mseb.2006.06.021

[20] Z.A. Motlagh, M.E. Azim Araghi. Mater. Sci. Semicond. Process., **40**, 701 (2015). DOI: 10.1016/j.mssp.2015.07.039

[21] S.Espevik, W. Chen-ho, R. H. Bube. J. Appl. Phys., **42**(9), 3513 (1971). DOI: 10.1063/1.1660763

[22] L.N. Neustroev, V.V. Osipov. FTP, **18** (2), 359 (1984) (in Russian).

[23] M. Kul. Anadolu Univ. J. Sci. Technol. (b), **7** (1), 46 (2019).

[24] G. M. Wolten. J. Electrochem. Soc., **122** (8), 1149 (1975). DOI: 10.1149/1.2134413

[25] I.S. Torriani, M.Tomyiama, S. Bilac, G.B. Rego, J.I. Cisneros, Z.P. Argüello. Thin Solid Films, **77**(4), 347 (1981). DOI: 10.1016/0040-6090(81)90328-X

[26] M. Sasani Ghamsari, M. Khosravi Araghi. Iran J. Sci. Technol. Trans. A, **29** (1), 151 (2005). DOI: 10.22099/ijsts.2005.2793

[27] I. Pop, V. Ionescu, C. Nascu, V. Vomir, R. Grecu, E. Indrera. Thin Solid Films, **283** (1−2), 119 (1996). DOI: 10.1016/0040-6090(95)08242-5

[28] L.N. Maskaeva, V. F. Markov, E.V. Mostovshchikova, V.I. Voronin, A.V. Pozdin, S. Santra. J. Alloys Compd., **766**, 402 (2018). DOI: 10.1016/j.jallcom.2018.06.263

[29] L.N. Maskaeva, E.V. Mostovshchikova, V.I. Voronin, E.E. Lekomtseva, P.S. Bogatova, V.F. Markov. Semiconductors., **54** (10), 12 (2020). DOI: 10.1134/S1063782620100231230-1240.

[30] V.G. Butkevitch, E.R. Globus, I.N. Zalevskai. J. Appl. Phys. **2**, (1999).

[31] A.N. Aleshin, A.V. Burlak, A.V. Ignatov, V.A. Pasternak, A.V. Tyurin. Mater. Transl. Neorg. Mater., **31**, 394 (1995).

[32] E.M. Larramendi, O. Calzadilla, A. Gonzalez-Arias, E. Hernandez, J. Ruiz-Garcia. Thin Solid Films, **389** (1−2), 301 (2001). DOI: 10.1016/s0040-6090(01)00815-x

[33] V.F. Markov, L.N. Maskaeva, E.V. Mostovshchikova, V.I. Voronin, A.V. Pozdin, A.V. Beltseva, I.O. Selyanin, I.V. Baklanova. PCCP, **24**, 16085 (2022). DOI: 10.1039/D2CP01815B

[34] R.L. Petritz. Phys. Rev., **104**, 1508 (1956).

[35] G.H. Blount, R.H. Bube, A.L. Robinson. J. Appl. Phys., **41**(5), 2190 (1970). DOI: 10.1063/1.1659188

[36] E. Indrea, A. Barbu. In: *2nd ht. Conj: on Photoexcited Processes and Applications* (ICPEPA-2, 1995), p. 37. DOI: 10.1016/S0169-4332(97)80012-8

[37] R. Candee, D. Dadarlat, P. Fitori, R. Turku, E. Indream, A. Darabont, L. Biro, I. Bratu, N. Aldea. Stud. Cercet. Fiz., **38**, 410 (1986).

[38] H.N. Acharya, H.N. Bose. Indian J. Phys., **54A**, 6 (1979).

[39] G.V. Samsonov, S.V. Drozdova. *Sulfidy* (Metallurgiya, M., 1972) (in Russian).

[40] R.H. Bube. *Photoconductivity in solids* (Wiley, NY., 1960).

[41] A.V. Burlak, V.V. Zotov, A.V. Ignatov. Poverkhnost. Fisika, khimiya, mekhanika **2**, 121 (1992). (in Russian)

[42] H.S.H. Mohamed, M. Abdel-Hafiez, B.N. Miroshnikov, A.D. Barinov, I.N. Miroshnikova. Mater. Sci. Semicond. Process., **27**, 725 (2014). DOI: 10.1016/j.mssp.2014.08.010

[43] L.N. Neustroev, V.V. Osipov. FTP, **21** (12), 2159 (1987) (in Russian).

[44] T.B. Fedorova, A.V. Vishnyakov, P.V. Kovtunenko. Issledovaniya v oblasti khimii i khimicheskoi tekhnologii materialov dlya elektronnoi tekhniki, **133**, 73 (1978) (in Russian).

[45] D. Vankhade, T.K. Chaudhur. Opt. Mater., **98**, 109491 (2019). DOI: 10.1016/j.optmat.2019.109491

[46] J. M. C. da Silva Filho, F.C. Marque. Mater. Sci. Semicond. Process., **91**, 188 (2019). DOI: 10.1016/j.mssp.2018.11.029

[47] M. Hangyo, S. Nakashima, Y. Hamada, T. Nishio, Y. Ohno. Phys. Rev. B, **48**(15), 11291 (1993). DOI: 10.1103/physrevb.48.11291

[48] R.G. Perez, G.H. Tellez, U.P. Rosas, A.M. Torres, J.H. Tecorralco, L.C. Lima, O.P. Moreno. J. Mater. Sci. Eng. A, **3**, 1 (2013).

[49] R. Sherwin, R.J.H. Clark, R. Lauck, M. Cardona. Sol. St. Commun., **134**(8), 565 (2005). DOI: 10.1016/j.ssc.2005.02.026

[50] T. Tohidi, K. Jamshidi-Ghaleh, A. Namdar, Abdi-Ghaleh. Mater. Sci. Semicond. Process., **25**, 197 (2014). DOI: 10.1016/j.mssp.2013.11.028

[51] T.D. Krauss, F.W. Wise, D.B. Tanner. Phys. Rev. Lett., **76**, 1376 (1996).

[52] S.V. Ovsyannikov, V.V. Shchennikov, A. Cantarero, A. Cros, A.N. Titov. Mater. Sci. Eng. A, **462**, 422 (2007). DOI: 10.1016/j.msea.2006.05.175

[53] M. Cortez-Valadez, A. Vargas-Ortiz, L. Rojas-Blanco, H. Arizpe-Chavez, M. Flores-Acosta, R. Ramirez-Bon. Phys. E, **53**, 146 (2013). DOI: 10.1016/j.physe.2013.05.006

[54] Y. Batonneau, C. Bremard, J. Laureyns, J. C. Merli. J. Raman Spectrosc., **31** (12), 1113 (2000). DOI: 10.1002/1097-4555(200012)31:12¡1113::aid-jrs653¿3.0.co;2-e

[55] K. Nakamoto. *IK spectry i spektry KR neorganicheskikh i koordinatsionnykh soedinenii* (Mir, M., 1991) (in Russian).

[56] R.A. Nyquist, R.C. Kagel. *Infrared Spectra of Inorganic Compounds (3800−45 cm⁻¹)* (Academic Press, NY., 1971).

[57] G.L.J. Trettenhahn, G.E. Nauer, A. Neckel. Vibr. Spectrosc., **5** (1), 85 (1993). DOI: 10.1016/0924-2031(93)87058-2

[58] M.H. Brooker. Can. J. Chem., **61**(3), 494 (1983). DOI: 10.1139/v83-087

[59] L. Little. *Infrakrasnye spektry adsorbirovannykh molekul* (Mir, Moscow, 1969) (in Russian).

[60] Ya.M. Grigoriev, D.V. Pozdnyakov, V.N. Filimonov. Russian Journal of Physical Chemistry, **46** (2), 316 (1972).

[61] L. Bellami. *Infrakrasnye spektry slozhnykh molekul* (IL, M., 1963) (in Russian).

[62] G.-U. Gremlih. *Yazyk spektrov. Vvedenie v interpretatsiyu spektrov organicheskikh soedinenii* (Optic, Bruker, 2002) (in Russian).

[63] O.H. Ellestad. Acta Chem. Scand. B, **35** (3), 155 (1981). DOI: 10.3891/acta.chem.scand.35a-0155

Translated by M.Shevelev